Applied Mathematical Modelling 125 (2024) 59–81

Contents lists available at ScienceDirect

Applied Mathematical Modelling

journal homepage: www.elsevier.com/locate/apm

Hyperreduced-order modeling of thermally coupled flows

Nicolás Espinoza-Contreras [a], Camilo Bayona-Roa [b], Ernesto Castillo [a,*], Tomás Gándara [a], Nelson O. Moraga [c]

[a] Departamento de Ingeniería Mecánica, Universidad de Santiago de Chile, Avenida Libertador Bernardo O Higgins 3363, Santiago, Chile
[b] Departamento de Ingeniería Industrial, Facultad de Ingeniería, Pontificia Universidad Javeriana, Bogotá, Colombia
[c] Universidad de La Serena, Departamento de Ingeniería Mecánica, Benavente 980, La Serena, Chile

ARTICLE INFO

Keywords:
Reduced-order modeling
Hyperreduction
Natural convection
Conjugate heat transfer
Stabilized finite element method

ABSTRACT

This article presents a full and reduced-order methodology based on the finite element method that allows the characterization of convective-dominant conjugate heat transfer flows. Reduced-order modeling (ROM) allows the description of several degrees of freedom problems, referred to as full-order modeling (FOM), through a reduced-order surrogate representation based on a Petrov-Galerkin projection onto a reduced subspace. The FOM and ROM problems are stabilized through the Variational Multi-Scale (VMS) method, which ensures stability in dominant convective problems and allows equal interpolation spaces for the pressure, velocity, and temperature. The proposed methodology is validated solving natural heat convection in a differentially heated square cavity, considering air as the working fluid and Rayleigh numbers in the interval $10^4 \leq Ra \leq 10^8$. In this problem, the benefit of using a ROM approximation for the three unknown fields, i.e., velocity, pressure, and temperature, is compared against ROM approximation only in the velocity and pressure fields and a FOM type approximation for temperature. The benefit of using mesh-based hyperreduction and its computational performance and precision are also analyzed. Subsequently, the method simulates a conjugate heat transfer problem that includes natural heat convection, allowing the inclusion of different rheologies between the working fluids. The results verify the precision and speed up of the calculations by more than three hundred times with respect to the time necessary to solve a full-order formulation, emerging it as a great potential tool in the resolution of thermally coupled flows.

1. Introduction

The conjugate heat transfer between two fluids separated by a solid container is common to a large number of applications in engineering, especially when an inner fluid is heated or cooled through the other to obtain a desired operating condition [1–4]. The heat transfer occurring in the outer domain can be related to forced, natural, or mixed heat convection, while in the interior, the heat transfer mechanism is carried out by natural convection.

In forced heat convection of incompressible flows, the temperature is a variable transported by velocity, with no explicit coupling between the Navier-Stokes equations and the thermal energy equation when density and viscosity are not changing with temperature. In this condition, the Navier-Stokes equations and energy can be solved sequentially without affecting the stability and precision of

* Corresponding author.
E-mail address: ernesto.castillode@usach.cl (E. Castillo).

https://doi.org/10.1016/j.apm.2023.08.028
Received 22 April 2023; Received in revised form 14 August 2023; Accepted 17 August 2023

Available online 24 August 2023

the solution [4–6]. In the natural convection of incompressible fluids, fluid-thermal coupling employing buoyancy forces is inevitable, and the inclusion of decoupling and iteration algorithms is necessary when Rayleigh numbers are high [7–9]. The design of efficient numerical schemes is a subject of high scientific and technological interest due to the high computational cost.

The precise calculation of heat transfer coefficients is of engineering interest in different industrial applications. It is a determining factor that defines the properties and the quality of heat-treated products [10–13]. Additionally, the energy required in the cooling or heating process strongly depends on the operating conditions to achieve the high quality required for foods. Development of efficient calculation tools to estimate these coefficients, particularly the Nusselt number, is necessary and has technological potential in the food [9,14,15], energy [16–18], electronic [1,4,6], and mechanical industries [19,20], among others. In this work, conjugate heat transfer problems refer to the sterilization processes of food, considering natural heat convection mechanisms in liquid foods. The sterilization problem serves to test the proposed methodology.

Most liquid foods show non-Newtonian rheological behavior [21]. Among the viscosity models most commonly used in numerical simulation, the purely viscous and viscoplastic types with shear-thinning characteristics are adopted in the food industry [15,22]. Incorporating these models in the governing equations increases the problem nonlinearity through the dependence on the viscosity to the velocity gradients. Including robust linearization schemes, stable discretization methods, and linear solvers capable of inverting poorly conditioned matrices is a topic of intense research [23–25].

The numerical approximation to solve thermally coupled incompressible flows for non-Newtonian fluids in simple geometries, such as square and rectangular cavities with imposed temperatures, has been a typical verification problem for new numerical methods in a wide range of Rayleigh numbers between $10^3 \leq Ra \leq 10^{10}$ [8,26–28]. The effect of the aspect ratio, Prandtl number, or the rheological character of the fluid have also been studied [7,29–31]. Regarding these aspects, the literature covers the size of the discretization, in time and space, necessary to achieve a high-fidelity description of the physics in the problems [32–34].

The numerical approximation of dominant convective flows, isothermal or thermally coupled, requires stabilization techniques to control spurious oscillations. These usually add some numerical dissipation to the solution. In the context of finite volumes and finite differences, the Upwind, Power-Law, QUICK, and TVD schemes, among others, are widely known [35,36]. Stabilized methods such as SUPG, GLS, and VMS, to name a few, are used to ensure the stability of the convective terms when the finite element method is used [37,38]. Additionally, compatibility constraints between velocity and pressure interpolation can be overcome with similar approaches.

One of the main barriers when carrying out simulations of practical applications is the long calculation time needed when using standard discretization methodologies, either the finite element method, the finite volume method, or the finite difference method, to name a few. That is especially true when solving nonlinear and time-dependent problems. In addition, for the conjugate heat transfer problem, large amounts of information are stored due to the multiple unknowns involved. In this context, reduced-order modeling (ROM) techniques are an efficient alternative that significantly reduces calculation times while preserving the quality of the full-order solutions [39–42]. Similar to full-order approximations, the stability of ROM schemes is challenging. In this regard, stabilization methods or closure models are decisive, as can be found in [43–47] and the references mentioned in those works.

Reduced-order modeling uses information from a full-order approximation, either from a finite element solution, finite volumes, or another discretization methodology. That information constructs the reduced basis through mathematical techniques such as proper orthogonal decomposition (POD), calculating the eigenvectors from singular vector decomposition (SVD) during the *online* stage. Later, in an *offline* stage, the basis generated by the POD technique is used to calculate new solutions using the same mesh from the FOM problem, known as reduced order modeling (ROM), or using a coarser mesh, known as mesh-based Hyperreduced Order Modeling or Hyper-ROM.

Hyperreduction encompasses approximating a projection-based reduced-order operator on a coarse mesh using a numerical algorithm to exploit the accuracy and stability of the projection-based reduced-order model. In computational mechanics, two primary approaches have emerged for achieving hyperreduction. The first approach revolves around utilizing the empirical interpolation method (EIM) [48,49], which has demonstrated success in computational fluid dynamics. EIM and its kindred techniques aim to approximate high-dimensional nonlinear functions by expanding them within a suitably reduced basis. Therefore, these techniques can be interpreted as analogous to high-dimensional interpolation schemes [50]. Hyperreduction involves a project-then-approximate paradigm, primarily developed within the finite element (FE) context. Within this framework, methods such as the reduced integration domain (RID) [51], generalized cubature [52], energy-conserving sampling and weighting (ECSW) [53], as well as mesh-based hyper-reduction methods [45], have been developed, and are examples of the second approach. Notably, these methods emphasize a sequential projection process, leading to the reduced model approximation. A comprehensive comparison between POD-Galerkin and POD-DEIM approaches for the incompressible Navier-Stokes equations is elaborated upon in [54]. The benefit of employing Hyper-ROM lies in the reduced computation time and the minimization of disk memory required to solve the problem and post-processing the solutions. However, it's worth noting that Hyper-ROM can result in a trade-off: while it accelerates computations, it might entail a loss in approximation resolution, consequently imposing a lower limit on the feasible mesh size needed to represent the physical problem with the desired level of accuracy.

Reduced-order methods are less often found in thermally coupled problems than in isothermal problems. In [55], the combining of direct numerical simulation databases and a closure model was proposed and verified to improve the evolution process of POD-ROM computations for the Rayleigh-Benard square cavity up to ($Ra = 10^7$). In [56], the classic natural convection reference problem on a differentially heated square cavity for stationary solutions up to a Grashof number ($Gr = 10^5$) has been considered with a Prandtl number equal to one and performed parametric calculations. The reduced approximations accelerate or *Speed-Up* the computation by three orders of magnitude compared to the full-order approximation. In [57], a VMS-Smagorinsky model for natural convection on the square cavity problem in the range $10^3 \leq Ra \leq 10^6$ included geometric parameterization based on the cavity height. In [43], search

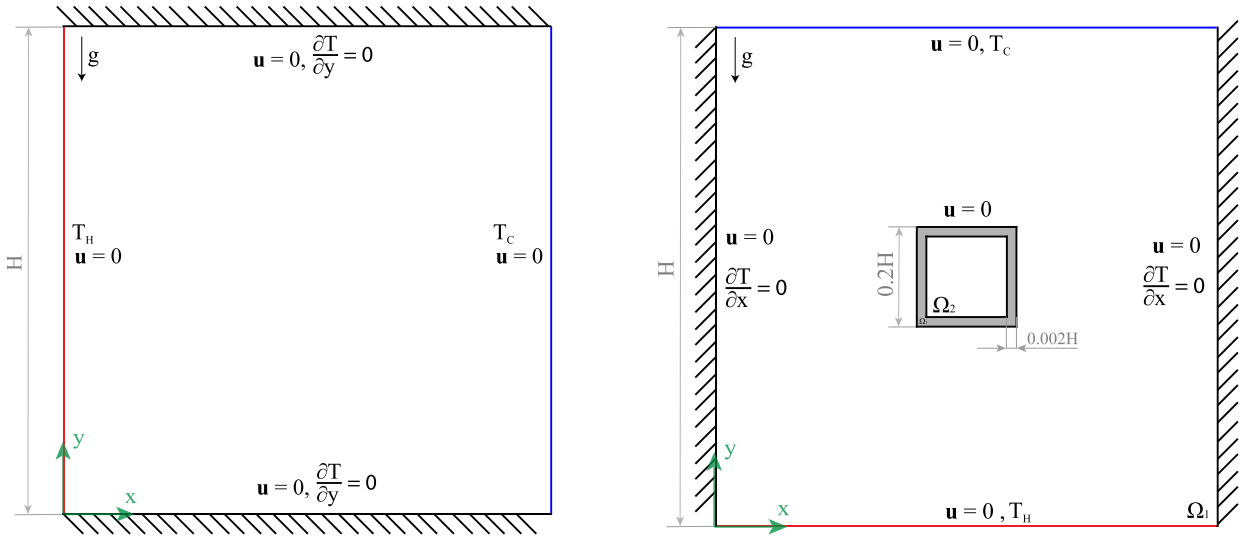

(a) Natural convection in a single domain.

(b) Multidomain natural convection.

Fig. 1. Schematics of the natural convection cases in a single domain and multiple domains.

techniques and reduced-order models that include Lyapunov's control theory solved the parametric calculation of natural convection. In [58], using the finite element method, a hyperreduction technique based on mesh coarsening is proposed for the thermally coupled *low-Mach* problem. In [59], a VMS-FOM/ROM formulation allows Hyper-ROM and adaptive meshes for Newtonian incompressible flows, including natural convection through the Boussinesq approximation. The results of that work show that using stabilization is vital for reduced approximations, unifying the idea of VMS stabilization for FOM and ROM.

The novelty of this work is the application of the VMS-ROM formulation in thermally coupled problems involving conjugate heat transfer. The solved problems consider two different fluids: one of them a generalized Newtonian and the other a Newtonian, as well as a solid that separates them apart. Regarding the numerical methodology, a unified FOM, ROM, and Hyper-ROM stabilized approach is detailed. The work includes numerical tests that evaluate the accuracy and performance of the ROM and Hyper-ROM approximations applied to only the velocity and pressure fields concerning the application of reduction methodologies for all the unknowns.

The structure of this paper is indicated next. The physical description of the problem is presented in Section 2. The governing equations and numerical strategy are provided in Section 3. The stabilization method used for FOM and ROM is described in Section 4. The description of the ROM method used is provided in Section 5. The numerical results are presented, analyzed, and discussed in Section 6. Finally, the conclusions of the work are drawn in Section 7.

2. Definition of the problem

In this work, we solve two problems involving heat transfer by natural convection.

1. The first one, outlined in Fig. 1-a), is the differentially heated square cavity benchmark. The cavity has Dirichlet vertical walls for temperature (one hot and one cold) and adiabatic horizontal walls. The fluid flow is with Rayleigh numbers in the range $10^4 \leq \mathrm{Ra} \leq 10^8$ and a Prandtl number of $\mathrm{Pr} = 0.71$.
2. The second problem, outlined in Fig. 1-b), is a conjugate heat transfer problem composed of two different fluids separated by a solid container. This problem is a simplified case of canned food sterilization. The boundary conditions at the outer domain of this problem are temperature imposed on the horizontal walls, hot in the lower and cold in the upper zones, and adiabatic vertical walls. In this problem, the outer fluid is water, while the inner fluid is a water-based food with shear-thinning rheological properties. The solid container has thick conductive walls made of aluminum for all cases. Two Rayleigh numbers of $\mathrm{Ra} = 10^4$ and $\mathrm{Ra} = 10^5$ are investigated for this problem case.

In Fig. 1, dimensions based on the size of the outer domain $H = 1$, and boundary conditions of the two problems are detailed with T_H as the hot temperature, and T_C being the cold temperature. Non-slip boundary conditions are imposed at all walls. The problem is composed of three subdomains: the outer fluid (Ω_1), the inner fluid (Ω_2), and the solid (Ω_3). The properties of each of the materials are detailed in Table 1, written in a dimensionless form, with water considered as the baseline material. That is, $\rho = 2.76$ indicates that the density of the solid is 2.76 times that of water, following the same logic for the other properties. Here, c_p is the specific heat, and k is the thermal conductivity. The parameters m and n are the consistency and power indices of the fluids.

Table 1
Thermophysical properties of fluids and solids.

	ρ	c_p	k	m	n
Fluid 1 (Ω_1),	1	1	1	6.9	1
Fluid 2 (Ω_2),	1	1	1	6.9	0.75
Solid (Ω_3),	2.76	0.22	337.9	-	-

3. Governing equations and models

Because the problems involve more than one material, the properties in the governing equations carry a subindex i. The subindex $i = 1$ is the outer fluid, $i = 2$ represents the inner fluid, and $i = 3$ is the solid, with the subindices being consistent with the definition of properties in Table 1. The case for a single fluid is without the index i. Considering this nomenclature, the equations to be solved are the Navier-Stokes equations coupled with the energy equation, which are defined below.

Let $\Omega \in \mathcal{R}^2$ be a two-dimensional domain bounded by the boundary $\partial\Omega$, through which a fluid flows in a time interval $(0, t_f)$. Additionally, the problem includes multiple materials. We can define $\Omega = \Omega_1 \cup \Omega_2 \cup \Omega_3$. Each domain is delimited by its boundaries $\partial\Omega_i$, some belonging to more than one material. Additionally, for all fluids, temperature is a common coupling variable. The convective term of the energy equation is neglected in the solid wall of the inner container, neither solving the Navier-Stokes equations. The system of coupled equations that governs the problem is:

$$\rho_i \frac{\partial \boldsymbol{u}_i}{\partial t} + \rho_i \boldsymbol{u}_i \cdot \nabla \boldsymbol{u}_i - \nabla \cdot (2\eta(\boldsymbol{u}_i)\nabla^s \boldsymbol{u}_i) + \nabla p_i = \boldsymbol{f}_i, \quad \text{in } \Omega_i,\ t \in (0, t_f), \tag{1}$$

$$\nabla \cdot \boldsymbol{u}_i = 0, \quad \text{in } \Omega_i,\ t \in (0, t_f), \tag{2}$$

$$\rho_i c_{pi} \frac{\partial T_i}{\partial t} + \gamma_f \rho_i c_{pi} \boldsymbol{u}_i \cdot \nabla T_i - k_i \Delta T_i = Q_i, \quad \text{in } \Omega_i,\ t \in (0, t_f), \tag{3}$$

where $\boldsymbol{u}_i$ represents the velocity, p_i is the pressure, and T_i is the temperature. Note that the energy equation includes the parameter γ_f of value 1 when the domain corresponds to that of a fluid and of value 0 in the solid. The properties of materials are the density ρ_i, the specific heat c_{pi}, the thermal conductivity k_i, and the apparent viscosity $\eta(\boldsymbol{u}_i)$. The volumetric force terms $\boldsymbol{f}_i$ and Q_i are included on the right-hand side of the momentum and energy equations, respectively. Using the Boussinesq approximation, we can calculate the buoyancy forces as, $\boldsymbol{f}_i = \rho_i \boldsymbol{g} \beta_i (T_i - T_{ref})$, where $\boldsymbol{g}$ is the acceleration of gravity, β_i is the coefficient of thermal expansion of fluids and T_{ref} is a reference temperature, used as the average between the T_H and T_C temperatures. Note that the bold notation corresponds to vectors and tensors.

The rheological model for the Newtonian and power-law fluids with shear-thinning characteristics is through the apparent viscosity defined as

$$\eta(\boldsymbol{u}) = m_i \dot{\gamma}^{n_i - 1}, \tag{4}$$

where $\dot{\gamma} = \sqrt{\frac{1}{2}(\dot{\boldsymbol{\gamma}} : \dot{\boldsymbol{\gamma}})}$ represents the magnitude of the strain-rate tensor $\dot{\boldsymbol{\gamma}} = \nabla \boldsymbol{u} + (\nabla \boldsymbol{u})^T$. As constitutive parameters of the model, m represents the consistency coefficient of the fluid with units $[Pa \cdot s^n]$ and n is the power index of the fluid. For $n > 1$, the fluid is called dilatant or shear-thickening; when $n < 1$, the fluid is known as pseudoplastic or shear-thinning; for $n = 1$ the Newtonian behavior is recovered. When using the power-law model, the appearance of apparent viscosity values may tend to zero or infinity when $\dot{\gamma}$ is closer to zero or take high values, respectively. A solution to that problem is implementing an upper and lower cut-off parameter so that the apparent viscosity is always limited. This work limits the apparent viscosity modulus to the interval $|m| / 10,000 \leq |\eta(\boldsymbol{u})| \leq 10,000\,|m|$.

This work studies thermally coupled flows of power-law fluids. The dimensionless numbers that characterize the flow cases are defined in a general way, recovering the Newtonian definitions when $n = 1$ and $m = \mu$, where μ is the kinematic viscosity of the fluid. The Reynolds, Prandtl, and Rayleigh numbers are defined as follows:

$$\mathrm{Re} = \frac{\rho U^{2-n} H^n}{m},\ \mathrm{Pr} = \frac{m k^{n-2} H^{2-2n}}{c_p^{n-2} \rho^{n-1}},\ \mathrm{Ra} = \frac{\beta g \rho^{n+1} c_p^n H^{2n+1} \Delta T}{m k^n}, \tag{5}$$

where H and ΔT represent a characteristic length and a characteristic temperature difference of the problem, respectively.

In the differentially heated cavity, the scaling velocity and temperature are $u^* = u/\sqrt{g\beta\Delta T H}$ and $T^* = (T - T_C)/(T_H - T_C)$, respectively, allowing to compare different dimensionless solutions related to Rayleigh numbers.

The mean Nusselt number on a wall is defined as

$$\overline{\mathrm{Nu}} = -\frac{1}{T_H - T_C} \int_0^{L_c} \frac{\partial T}{\partial \mathbf{n}}\, ds, \tag{6}$$

where L_c represents the length of the wall, ds the differential length surface, and $\mathbf{n}$ is the normal unit vector.

3.1. Variational formulation and Galerkin's problem

Using a standard notation helps to define the weak form of the problem. The space of bounded and integrable square functions on a domain Ω is defined by $L^2(\Omega)$. The space of functions whose distributional derivative of the first order belongs to the $L^2(\Omega)$ space is denoted by $\mathcal{H}^1(\Omega)$. The space $\mathcal{H}^1_0(\Omega)$ is composed of functions belonging to $\mathcal{H}^1(\Omega)$ that vanish at the boundaries. The inner product of two functions is $\langle\cdot,\cdot\rangle$. When the functions belong to the $L^2(\Omega)$ space, then $\langle\cdot,\cdot\rangle = (\cdot,\cdot)$.

Using this notation, the spaces for the velocity, pressure, and temperature vector are defined as $\boldsymbol{\mathcal{V}} = \mathcal{H}^1_0(\Omega)^2$, $\mathcal{Q} = L^2(\Omega)/\mathbb{R}$, and $\Theta = \mathcal{H}^1_0(\Omega)$, respectively. If we define $\boldsymbol{\mathcal{Y}} := \boldsymbol{\mathcal{V}} \times \mathcal{Q} \times \Theta$, the weak form of the problem consists of finding $\boldsymbol{y} = [\boldsymbol{u}, p, T] : (0, t_f) \to \boldsymbol{\mathcal{Y}}$ such that

$$\left(\rho\frac{\partial \boldsymbol{u}}{\partial t}, \boldsymbol{v}\right) + \langle \rho\boldsymbol{u}\cdot\nabla\boldsymbol{u}, \boldsymbol{v}\rangle + 2\eta(\boldsymbol{u})(\nabla^s\boldsymbol{u}, \nabla^s\boldsymbol{v}) - (p, \nabla\cdot\boldsymbol{v}) = \langle \boldsymbol{f}, \boldsymbol{v}\rangle, \tag{7}$$

$$(\nabla\cdot\boldsymbol{u}, q) = 0, \tag{8}$$

$$\left(\rho c_p\frac{\partial T}{\partial t}, \theta\right) + \rho c_p\langle \boldsymbol{u}\cdot\nabla T, \theta\rangle + k(\nabla T, \nabla\theta) = \langle Q, \theta\rangle, \tag{9}$$

for all $[\boldsymbol{v}, q, \theta] \in \boldsymbol{\mathcal{Y}}$, assuming that $\boldsymbol{f}$ and Q are well defined. The previous equations are written without the material subindex or the parameter γ_f to avoid over-notation.

The previously defined problem can be written compactly as

$$\left(\rho\frac{\partial \boldsymbol{u}}{\partial t}, \boldsymbol{v}\right) + \left(\rho c_p\frac{\partial T}{\partial t}, \theta\right) + B(\hat{\boldsymbol{u}}; \boldsymbol{y}, \boldsymbol{\psi}) = \langle \boldsymbol{f}, \boldsymbol{v}\rangle + \langle Q, \theta\rangle, \quad \forall \boldsymbol{\psi} = [\boldsymbol{v}, q, \theta] \in \boldsymbol{\mathcal{Y}}, \tag{10}$$

where

$$B(\hat{\boldsymbol{u}}; \boldsymbol{y}, \boldsymbol{\psi}) = \langle \rho\hat{\boldsymbol{u}}\cdot\nabla\boldsymbol{u}, \boldsymbol{v}\rangle + 2\eta(\hat{\boldsymbol{u}})(\nabla^s\boldsymbol{u}, \nabla^s\boldsymbol{v}) - (p, \nabla\cdot\boldsymbol{v}) + (\nabla\cdot\boldsymbol{u}, q) + \rho c_p\langle \hat{\boldsymbol{u}}\cdot\nabla T, \theta\rangle + k(\nabla T, \nabla\theta). \tag{11}$$

In the definition of the $B(\hat{\boldsymbol{u}}; \boldsymbol{y}, \boldsymbol{\psi})$ operator, the variable $\hat{\boldsymbol{u}}$ is used to denote the advection velocity, which in the Navier-Stokes problem is the same velocity $\boldsymbol{u}$. However, when using finite elements and linear solvers, this velocity corresponds to the previous iteration employing fixed-point linearization.

Using conforming finite element spaces, $\boldsymbol{\mathcal{V}}_h \subset \boldsymbol{\mathcal{V}}$, $\mathcal{Q}_h \subset \mathcal{Q}$, $\Theta_h \subset \Theta$. If $\boldsymbol{\mathcal{Y}}_h := \boldsymbol{\mathcal{V}}_h \times \mathcal{Q}_h \times \Theta_h$ and $\boldsymbol{y}_h = [\boldsymbol{u}_h, p_h, T_h]$, the Galerkin problem consists of finding $\boldsymbol{y}_h = [\boldsymbol{u}_h, p_h, T_h] : (0, t_f) \to \boldsymbol{\mathcal{Y}}_h$, such that

$$\left(\rho\frac{\partial \boldsymbol{u}_h}{\partial t}, \boldsymbol{v}_h\right) + \left(\rho c_p\frac{\partial T_h}{\partial t}, \theta_h\right) + B(\hat{\boldsymbol{u}}_h; \boldsymbol{y}_h, \boldsymbol{\psi}_h) = \langle \boldsymbol{f}, \boldsymbol{v}_h\rangle + \langle Q, \theta_h\rangle, \quad \forall \boldsymbol{\psi}_h = [\boldsymbol{v}_h, q_h, \theta_h] \in \boldsymbol{\mathcal{Y}}_h, \tag{12}$$

satisfying the initial and boundary conditions of the problem.

For the time derivative of the equations of linear momentum and energy, a second-order backward differentiation scheme is used

$$\frac{\partial \phi_h^{j+1}}{\partial t} = \frac{3\phi_h^{j+1} - 4\phi_h^j + \phi_h^{j-1}}{2\delta t} + \mathcal{O}(\delta t^2), \tag{13}$$

where ϕ_h represents either velocity or temperature, δt corresponds to the time step in the interval $(0, t_f)$, considered as uniform, and $\mathcal{O}(\cdot)$ represents the order of approximation. The superscripts indicate the discrete time. Therefore, ϕ_h^j represents the approximation of the unknown function ϕ_h at the time step $t^j = j\delta t$.

4. Stabilized finite element method

The numerical approximation of dominant convective flows requires some numerical dissipation that ensures stability when the local Reynolds or Peclet numbers exceed two. Additionally, equal interpolation between velocity and pressure does not produce physically correct approximations without some stabilization mechanism.

In the VMS method, the space of approximation of the unknowns is broken down into two parts: a finite-dimensional space $\mathcal{Y}_h$ and its complement, called *Subscales* $\tilde{\mathcal{Y}}$ so that $\mathcal{Y} = \mathcal{Y}_h \oplus \tilde{\mathcal{Y}}$. The basic idea of this type of method consists of modeling the subscale as a function of the resolved scale. Thus, additional stabilizing terms in the Galerkin problem arising from the VMS formulation ensure stability in dominant convection and preserve the optimal convergence properties of the numerical method.

This work uses the term-by-term nonresidual VMS formulation proposed in [60] and verified numerically in [8,61,62] for isothermal and thermally coupled incompressible fluid flows. The notation for the stabilizing terms is similar to the one in these articles without referring to the design of the method. The stabilized problem consists of finding $\boldsymbol{y}_h = [\boldsymbol{u}_h, p_h, T_h] : (0, t_f) \to \boldsymbol{\mathcal{Y}}_h$ such that

$$\begin{aligned}\left(\rho\frac{\partial \boldsymbol{u}_h}{\partial t}, \boldsymbol{v}_h\right) + \left(\rho c_p\frac{\partial T_h}{\partial t}, \theta_h\right) + B(\hat{\boldsymbol{u}}_h; \boldsymbol{y}_h, \boldsymbol{\psi}_h) - \sum_K \tau_2(\hat{\boldsymbol{u}}_h)\left(\nabla\cdot\boldsymbol{v}_h, \mathcal{P}_h^\perp(\nabla\cdot\boldsymbol{u}_h)\right)_K \\ + \sum_K \boldsymbol{\tau}_1(\hat{\boldsymbol{u}}_h)\left(\nabla q_h, \mathcal{P}_h^\perp(\nabla p_h)\right)_K + \sum_K \boldsymbol{\tau}_1(\hat{\boldsymbol{u}}_h)\left(\hat{\boldsymbol{u}}_h\cdot\nabla\boldsymbol{v}_h, \mathcal{P}_h^\perp(\hat{\boldsymbol{u}}_h\cdot\nabla\boldsymbol{u}_h)\right)_K \\ + \sum_K \tau_3(\hat{\boldsymbol{u}}_h)\left(\rho c_p\hat{\boldsymbol{u}}_h\cdot\nabla\theta_h, \mathcal{P}_h^\perp(\rho c_p\hat{\boldsymbol{u}}_h\cdot\nabla T_h)\right)_K = \langle \boldsymbol{f}, \boldsymbol{v}_h\rangle + \langle Q, \theta_h\rangle,\end{aligned} \tag{14}$$